

Aerodynamics Analysis of F-16 Aircraft

HAM Peiris, PVS Nirmal[#], HMHHS Bandara, DM Mahindaratne,
SLMD Rangajeeva and RMPS Bandara
General Sir John Kotelawala Defence University, Ratmalana, Sri Lanka
[#]nirmal.pvs@gmail.com

Abstract— *The Lockheed Martin F-16 Fighting Falcon is the world's most prolific fighter with more than 2000 in service. The primary objective of this research project is to evaluate the aerodynamics behaviour of the F-16 aircraft by conducting Computational Fluid Dynamics (CFD) analysis. The CFD simulations have been done in both subsonic and supersonic flight regimes. As a means of validating the results, the CFD analysis has been done with two different turbulence models. A 1:1 CATIA solid model of F-16 aircraft was used to generate computational mesh and subsequent CFD simulations were performed mainly with Fluent ANSYS. During the post processing phase of the CFD results, the aerodynamic characteristics of the F-16 have been predicted in terms of lift coefficient and drag coefficient over angles of attack ranges from 0° to 40°. In comparing CFD predictions between turbulence models, a minimal variation of those dimensionless quantities was recorded. At Mach number 0.6, formation of two large leading edge vortices which is the subsonic lift generation mechanism, were observed on the main wings. A complete analysis of shock waves and expansion fans formation around the aircraft was also performed at supersonic speed, by examining the static pressure variation. Further to examine flow over main wings, the surface static pressure variation and pressure coefficient variation at different span-wise locations have been also studied. The flow physics revealed with CFD analysis are well aligned with both subsonic and supersonic theories. The forecasted values for aerodynamic efficacy and dimensionless parameters are lower than expected. It has been found this particular fact is directly related to computational limitations associated with CFD. The outcomes from this piece of research not only provides better sight to fine details about fluid dynamics in relation to F-16, but also made vital recommendations for future CFD analysis of F-16 aircraft.*

Keywords— *CFD, F-16 Aircraft, Turbulence Models*

I. INTRODUCTION

A. F16 Aircraft

With the technological advancement and 138 different configurations, the famed F-16 is the world's largely

operative 4th Generation multi-role fighter aircraft (Martin, 2015). The main goal of the designers of F-16 was to create a simpler with greater manoeuvrable fighter aircraft of the time. Their concepts challenged by the shape and the way it should fly. Finally they accomplished with the results of: a level blended-wing body with extra lift and control, a fly-by-wire system that kept the design stable, with better response time and increased its agility and an enhanced cockpit – including a tilted back ejection seat, side-mounted throttle and control stick, head-up display and bubble canopy with improved pilot survivability, visibility and control.

The Fighting Falcon is the cumulative results of F-16 pilots' combat experience and built on the primary strengths of the original Fighting Falcon design. With the time passes introducing new technologies into the cockpit, avionics, sensors and weapons, the aircraft has become more reliable, more maintainable and more supportable (Martin, 2015).

B. Computational Fluid Dynamics

Computational Fluid Dynamics (CFD) is the process of using computers to simulate realistic flows. In computer form, the geometry of aircraft designs can be readily defined and modified. CFD deals with the aerodynamicist a means of exploring variety of aircraft shapes than can usually be achieved, in available time scales. For the simulation the type of model should dependent on the accuracy needed, the computer power accessible and the time scale to accomplish the analysis. The central point of CFD problems is the Navier–Stokes equations which includes continuity, momentum and energy.

C. Turbulence Models

Turbulence models are generally classified according to which governing equations they apply. Furthermore they are classified by the number of additional transport equations which one must solve in order to compute the model contributions (Clelik, 1999).

One class of the turbulence models is the Reynolds-Averaged Navier-Stokes (RANS) model, and is used for

most production applications. Further this is categorized according to their usage of wall functions, the number of additional variables solved for and what these variables represent. All of these models augment the Navier-Stokes equations with an additional turbulent viscosity term (Jurij SODJA, 2007). But they differ in how it is computed. During the analysis process to resolve the details of the turbulent fluctuations, the solutions are focused on two turbulence models namely;

- a. Standard k-epsilon (ϵ) model
- b. Shear Stress Transport (SST) k-omega (ω) model

II. METHODOLOGY

A. Solid Modeling

The solid model was created using CATIA V5R18. The model was basically drawn with the aid of CATIA V5R16. Initially the different schematics views of F-16 Aircraft were downloaded from the web. Three Extrude surfaces were crated while offsetting from XY, YZ and ZX planes. Then the reference pictures were applied onto these three surfaces. Sketches were drawn to each and every cross section while relocating them into the correct positions. The Body, then the wing and finally the tail were created with using 3D curves and "Freeform" surfaces.

B. Mesh Generation

Second process was to develop a mesh as referred in Figure 1. In order to obtain valid and accurate results creating a fine mesh is important. Mesh was created using the software OpenFOAM with the use of "snappyHexMesh" commanding. Before creating the aircraft mesh the domain mesh was successfully created with the use of command "blockMesh". Modifications were created to define three refinement boxes which the first was covering whole aircraft, the second was covering the tail part of aircraft, and the third was covering the both wings. But to accommodate a mesh with more accuracy 5 layers were developed near to the aircraft surface. Another development had been made to create another block after the model till the end of domain where the flow is having its most critical phenomena such as turbulence, wakes and flow separation.

The number of nodes points and cells are as referred in the Table 1.

Table 1 - Mesh Features

Cells	Faces	Nodes	Partitions	Cell Zones	Face Zones
792571	2415081	830701	1	1	8

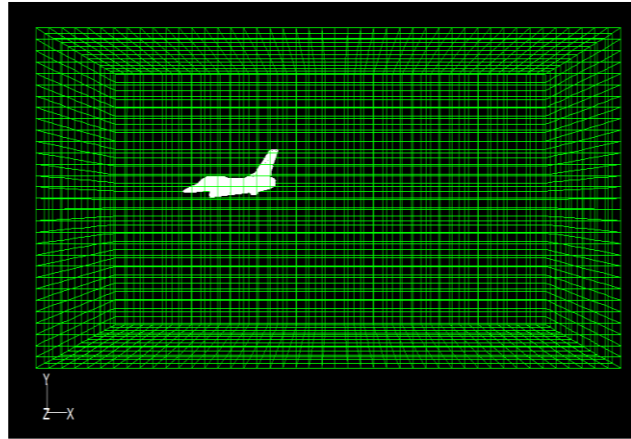


Figure 1 - Generated Mesh

C. Cfd Simulation

The simulation of continuum was done in ANSYS Fluent 14. In this initially the meshing of the continuum was read and then checked. Once the software approves it, the scale was selected in mm as the model was created and meshed using the unit mm. Then the models, materials and boundary conditions were set.

1) turbulence Models:

The turbulence models used for these simulations were the k- ϵ model and k- ω SST. The solver was based on "density based" as the all of the simulations were compressible. Energy equations were selected in order to solve the cases as all of the simulations were compressible.

2) Materials:

The working fluid in this simulation was ideal gas as the boundary condition "Pressure Far field" was compactible with it. It was considered the F-16 aircraft was flying at sea level conditions and the viscosity was solved using Sutherland equations.

3) Boundary Conditions:

Pressure far-field boundary conditions were used in this simulation to model a free-stream compressible Flow at infinity, with free-stream Mach number and static

conditions specified. The aircraft was given with “wall” boundary condition.

4) *Solution:*

The solver was semi-implicit method for pressure-linked equations (SIMPLE) algorithm. This algorithm is an iterative procedure for solving equations for velocity and pressure, for steady-state. The Courant number is set to 2 and the under relaxation factors for momentum and pressure are set as 0.5 and for the turbulent kinetic energy, turbulent dissipation rate and turbulent viscosity is set to 0.5. For the discretization the pressure was kept as standard, while the other parameters Momentum, Turbulent Kinetic Energy, Turbulent dissipation Rate and Energy were retained as Second Order Upwind.

Monitoring the convergence during the solution was dynamically checked by force coefficient values rather than checking for the convergence through residuals. The data were printed, reported and displayed in plots of lift, drag, and moment coefficients, and residuals for the solution variables. In the Force Monitors, the Force vectors Lift and Drag had to define with relative to the free stream direction.

5) *Reference Values:*

When calculating force coefficients the reference values should be given to get the actual results. So the Reference Values of area, length, pressure, density, temperature and velocities were given as 27.87m², 14.23 m, 101325 Pa, 1.225 kgm⁻³, 288.16 K, 204ms⁻¹ for subsonic (Mach 0.6) and 408ms⁻¹ for supersonic (Mach 1.2) respectively.

7) *Iterate:*

The numbers of iterations were set to 10000 to be performed in the Number of Iterations field. Then the FLUENT began with the calculations starting at iteration 1, using the initial solution. Then the graphs were plotted, printed and written (in separate data files). When the observations in the graphs of Coefficient of Lift Vs iterations and Coefficient of Drag Vs iterations were converged, the simulations were stopped.

III. RESULTS AND DISCUSSION

A. *Formation Of Wing Tip Vortices At M=0.6*

At Mach number 0.6, formation of two large leading edge vortices which is the subsonic lift generation mechanism, were observed on the main wings.

The subsonic (M=0.6) flow pattern over the top of a delta wing in F-16 aircraft at AOA=40° is as for the Figure 2 and

Figure 3. The dominant aspects of this flow are two vortex patterns that occur in the vicinity of the highly swept leading edges. These vortex patterns are created by the mechanism of the pressure on the bottom surface of the wing is higher than the pressure on the top surface. Thus, the flow on the bottom surface in the locality tries to curl around the leading edge from the bottom to the top.

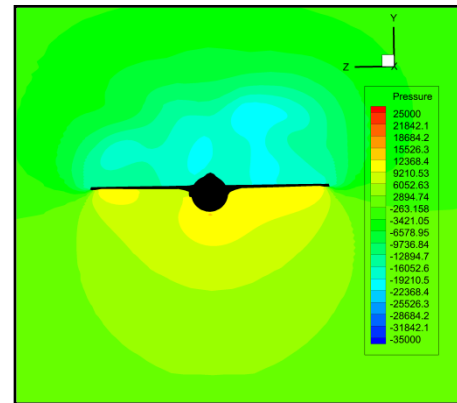


Figure 2 - Static pressure distribution over wing span

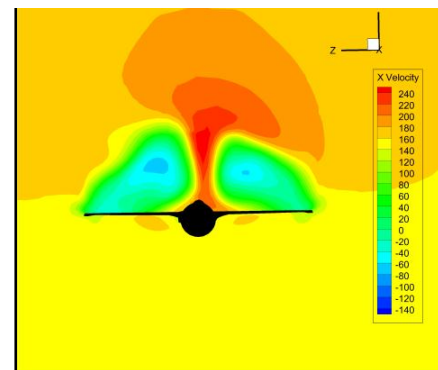


Figure 3 - Velocity distribution over wing span

The leading edge vortices are strong and stable. The local static pressure of the vortices is considerably dropped due to the high vorticity flow. The leading edge vortices are figuratively creating a strong “suction” on the top surface near the leading edges due to the pressure difference. The suction effect of the leading edge vortices increase the normal force which will enhance the lift. For this reason, the lift coefficient for a delta wing exhibits an increase in C_L for values of high angles of attack at which conventional wing planforms would be stalled.

Since delta-winged aircraft are performing in supersonic speeds in their missions; the aircraft has to perform in subsonic speeds in their landing and takeoff. So the low-speed aerodynamics of delta wings for F-16 aircraft is having a pronounced importance in lift generation mechanism at subsonic speeds (Anderson, 2013).

B. Shock Waves And Expansion Fans Around Aircraft At Mach=1.2

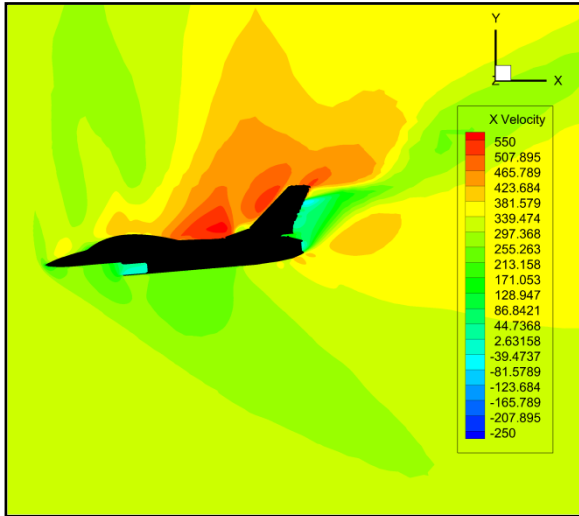


Figure 4 - Velocity distribution along axis of symmetry

Starting from nose and along the X- axis in the upper surface of the F-16 aircraft, three shock waves (as denoted with the locations “A”, “B” and “C” in Figure 5) were created with a clear variation of static pressure reduction, velocity and static temperature rise as for the Figure 5, Figure 4 and Figure 6 respectively. Again with ability to flow over a convex angle with the aircraft represented by location “D” as showed in the Figure 5 a series of expansion waves were found with satisfying the isentropic conditions. The properties of expansion waves are in a contradictory way to the flow properties of shock waves. The results can be interpreted as rise in velocity magnitude and reductions in static temperature as well as the static pressure as shown in the Figure 4, Figure 6 and Figure 5 respectively.

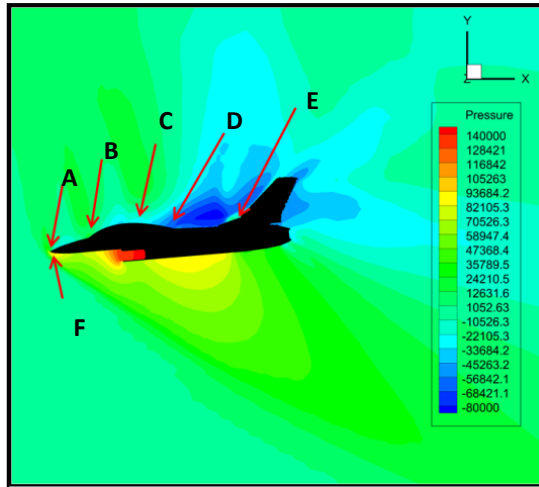


Figure 5- Pressure Distribution along axis of symmetry

The upswing of Mach number due to the expansion fan occurred in the upper surface of the aircraft body, another shockwave was arisen. So this oblique shock wave was formed in front of the vertical stabilizer on the body with the body, symbolized with the location “E” in Figure 5, signify a rise in static pressure while having a reduction in static temperature and velocity as for referenced figures respectively in order to retard the flow to obtain free stream conditions (Anderson, 2013).

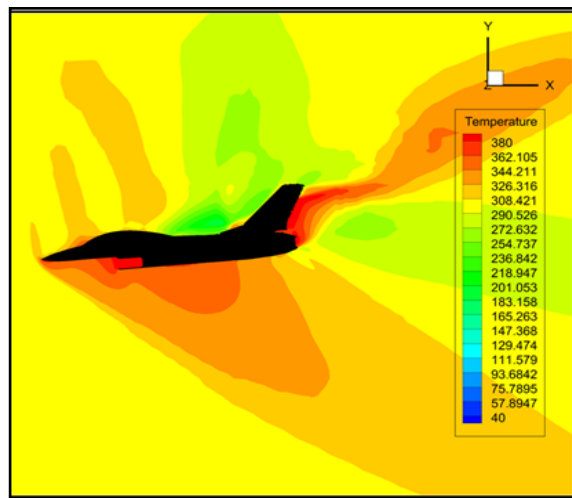


Figure 6 - Static temperature distribution along axis of symmetry

C. Lift Curve, Drag Curve, Drag Polar And Moment Curve

1) Lift Curve:

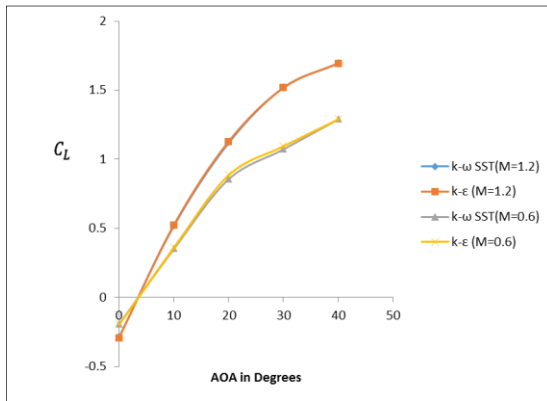


Figure 8- Coefficient of Lift Vs AOA

When considering the graph referred in Figure 8, it could identify that the flow over the upper surface of the airfoil is still not separated and it is in attached with the airfoil surface. Though the CFD gave a high AOA for the C_L max in practical the flight control system of the F-16 limits it up to 25.5°. It was because to reduce the high g force on the fighter pilots at their manoeuvres this was achieved by the Flight Control System installed in the F-16 aircraft.

2) Drag Curve:

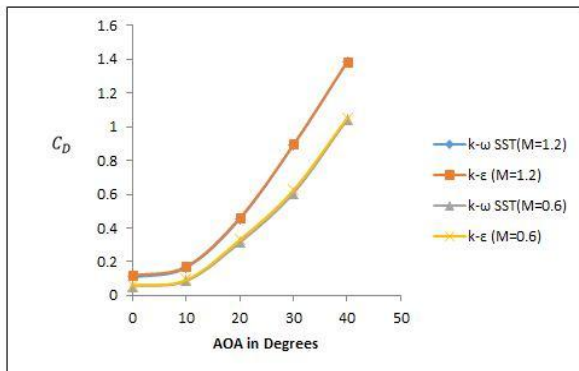


Figure 9- Coefficient of Drag Vs AOA

When consider the normal shape of the graphs we could see same change in graph of Figure 9. The value at zero angle of attack is little bit stationary and it is because for lower angles of attack the flow will not separate much over the airfoil. But when the angle of attack increases the flow will slightly separate from the upper surface of the airfoil. There the present of wakes are prominent than in lower angle of attacks. When the separation

become more and more one time the lift generate will not sufficient to bare the self-weight of the aircraft and will stall. At this time the coefficient of drag will be at the maximum.

3) Drag Polar

Drag Polar at M=0.6 for turbulence models of k- ϵ and k- ω SST as for the Figure 11. Here no clear difference between two graphs can be observed. The graph is according to the Equation (1), where $C_{D,0}$ the parasite drag coefficient at zero lift. $\frac{C_L^2}{\pi e AR}$ Value represents the parasite drag and induced drag due to lift. And also “e” is referred to the Oswald Efficiency Factor and “AR” is aspect ratio.

$$C_D = C_{D,0} + \frac{C_L^2}{\pi e AR} \quad (1)$$

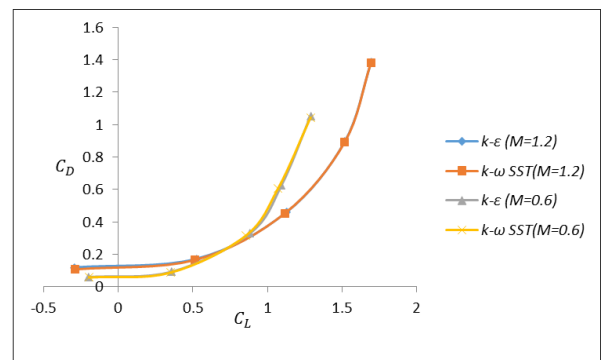


Figure 10- Drag polar

A comparison of drag polar at M=0.6 and M=1.2 for different turbulence models as for the Figure 11. With the increasing Mach number a distinct variation can be identified in the $C_{D,0}$ value at zero lift. The drag polar curves also have identical difference in different Mach numbers.

4) Lift To Drag Ratio Versus Angle Of Attack

The lift to drag ratio is measure of aerodynamic efficiency where the F-16 requires minimum thrust to operate. The maximum value for the C_L/C_D at M = 1.2 is smaller than that of the M = 0.6. It could be due to the high drag produced at high speeds. So the ultimate value for the value C_L/C_D is getting smaller and this maximum value is obtained at AOA= 13°. The results obtained for the values of maximum aerodynamic efficiencies are for the Table 2.

Table 2-Maximum aerodynamic efficiency values

Turbulence Models	Maximum aerodynamic efficiency	
	M=1.2	M=0.6
<i>k-ε</i>	3.15	4.2
<i>k-ω SST</i>	3.2	4.35

D. Flow Properties Over Different Span Wise Locations On The Wing

Velocity magnitude and static pressure variations over different span wise locations on the wing have been observed. From the axis of symmetry, the span wise locations 2m, 3m, and 4m on the wing were taken.

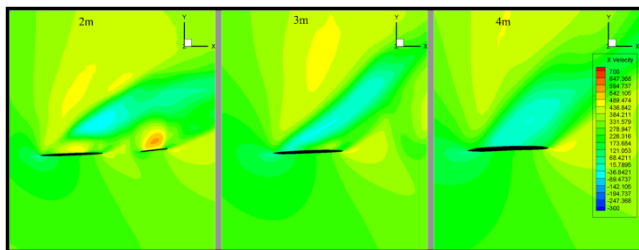


Figure 12- Velocity magnitude

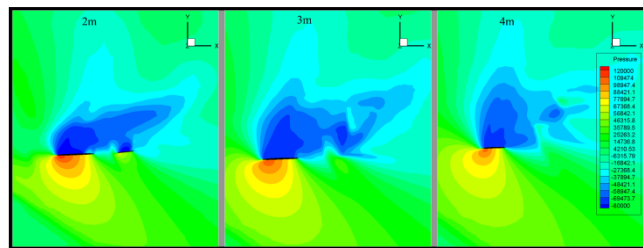


Figure 13- Pressure magnitude

With the distractions created with the whole aircraft body, the particular flow properties over the wing were unable to recognize properly. But with the distance from the axis of symmetry as for the Figure 12 and Figure 13 the flow properties on the wing was clearly detected. Shock waves on the leading edge of the wing were determined with the reduction of velocity magnitude and a rise of static pressure as highlighted in the Figure 12 and Figure 13. But comparing to the velocity variation, a slight variation of static pressure is observed.

IV. COCLUSION

This research project was evaluated the aerodynamics behavior of the F-16 aircraft by conducting Computational Fluid Dynamics (CFD) analysis while performing the CFD simulations in both subsonic and

supersonic flight regimes with two different turbulence models. During the post processing phase of the CFD results, the aerodynamic characteristics of the F-16 have been predicted in terms of lift coefficient and drag coefficient over angles of attack ranges from 0° to 40°. In comparing CFD predictions between turbulence models, a minimal variation of those dimensionless quantities was recorded. At Mach number 0.6, formation of two large leading edge vortices which is the subsonic lift generation mechanism, were observed on the main wings. The suction effect of the leading edge vortices enhances the lift coefficient for a delta wing exhibits for values of high angles of attack at which conventional wing planforms would be stalled. A series of shock waves in the upper surface as well as in the lower surface of the aircraft was observed with the drastic changes in flow properties such as rise in static pressure, reductions in flow velocity and rise in temperature. While expansion fans formation around the aircraft was also observed at supersonic speed, by examining the contradictory flow property changes to the shock waves such as rise in velocity, reductions in static pressure and temperature variation. Further the research was examined the flow over main wings, the surface static pressure variation and pressure coefficient variation at different span-wise locations. Due to the formation of shock waves with the static pressure rise, a higher adverse pressure gradient has been observed. The flow physics revealed with CFD analysis are well aligned with both subsonic and supersonic theories. The forecasted values for aerodynamic efficacy and dimensionless parameters are lower than expected. It has been found this particular fact is directly related to computational limitations associated with CFD.

REFERENCES

Anderson, J. D., 2013. *Fundamentals of Aerodynamics*. 5th ed. New York: Mc Graw Hill.

Anderson, J. D., 2013. *Introduction to Flight*. 6th ed. New York: Mc Graw-Hill.

Clelik, B. I., 1999. *Introductory Turbulence Modeling*, Morgantown: West Virginia University.

Jurij SODJA, R. P., 2007. *Turbulence Models in CFD*, s.l.: s.n.

Martin, L., 2015. *F-16 Fighting Falcon*. [Online] Available at: <http://usfighter.tripod.com/f16.htm> [Accessed 03 08 2014].